Dalton Transactions

PAPER

View Article Online
View Journal | View Issue

Cite this: *Dalton Trans.*, 2015, **44**, 15157

1,2,4-Triazole-derived carbene complexes of gold: characterization, solid-state aggregation and ligand disproportionation†

Shuai Guo, Jan Christopher Bernhammer and Han Vinh Huynh*

Received 17th October 2014,
Accepted 20th January 2015

DOI: 10.1039/c4dt03201b

www.rsc.org/dalton

Ligand redistribution reactions are well documented for silver(I) N-heterocyclic carbene (NHC) complexes of the type [AgX(NHC)] (X = halido ligand), but only two reports have been described in the literature for gold analogues of the general formula [AuX(NHC)]. In both cases, the NHCs in question were exceptionally strong donors. To probe the dependence of ligand redistribution processes on NHC donor strength, a model study was conducted using a weakly donating 1,2,4-triazolin-5-ylidene (tazy) ligand and different halido coligands. For [AuX(tazy)] (X = Cl, Br, OAc, tazy = 4-benzyl-1-methyl-1,2,4-triazolin-5-ylidene), no ligand redistribution was found, while a reversible disproportionation between [AuI(tazy)] in solution and $[Au(tazy)_2][AuI_2]$ in the solid state was observed and studied by means of X-ray crystallography, NMR and UV-Vis spectroscopy, as well as DFT calculations.

Introduction

Coinage metal complexes incorporating N-heterocyclic carbenes (NHCs) have received a great deal of interest[1] due to their intriguing coordination chemistry as well as their applications in catalysis,[2] luminescence,[3] and biological science.[4] In this context, much attention has been paid to Ag(I) mono-NHC complexes of the type [AgX(NHC)] (X = halido ligand), particularly due to their ability to serve as carbene transfer agents.[5] The structural diversity of silver NHC complexes in this category has proved to be fairly broad. A large number of neutral (*e.g.* [AgX(NHC)], $[AgX(NHC)]_2$) and ionic structures (*e.g.* $[Ag(NHC)_2][AgX_2]$) have been reported. Additionally, fluxional behaviour has been observed for different Ag–NHC species in solution, indicating rapid ligand disproportionations.[6]

In contrast, only scattered examples of ligand disproportionations of complexes with the general formula [AuX(NHC)] have been reported, although such complexes have been extensively employed in homogenous catalysis.[2] A DFT study by Frenking *et al.* has revealed that the bond dissociation energy (BDE) of group 11 metal–NHC bonds follows the trend Au > Cu > Ag.[7] The disproportionation process of complexes [AuX(NHC)], obviously involving the breakage and reconstruction of Au–$C_{carbene}$ bonds, is probably less favourable due to the higher BDE of the Au–NHC bond.

To the best of our knowledge, there are only two examples in this regard.[8] In 2008, Bertrand and co-workers reported an ionic complex $[Au(CAAC)_2][AuCl_2]$ (**A′**),[8a] which can be generated *via* the autoionization of the neutral complex [AuCl(CAAC)] (**A**) in solution (**I**, CAAC = 2-(2,6-diisopropylphenyl)-3,3-dimethyl-2-azaspiro[4.5]decan-1-ylidene, Scheme 1). In 2012, we published the 2nd example for ligand disproportionation, involving an indazole-derived carbene complex [AuI(Indy)] (**B**, Indy = 6,7,8,9-tetrahydropyridazino[1,2-*a*]indazolin-

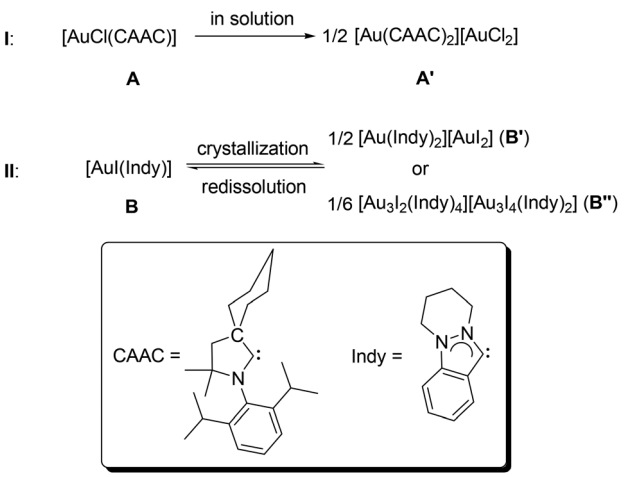

Scheme 1 Previous reports on ligand disproportionations of complexes of the type [AuX(NHC)] (X = halido ligand).

Department of Chemistry, National University of Singapore, 3 Science Drive 3, 117543 Singapore, Singapore. E-mail: chmhhv@nus.edu.sg; Fax: +65 6779 1691; Tel: +65 6516 2670

† Electronic supplementary information (ESI) available: Selected crystallographic data; Computational details. CCDC 1029440–1029445. For ESI and crystallographic data in CIF or other electronic format see DOI: 10.1039/c4dt03201b

3-ylidene).[8b] The latter was found to be solvent-dependant and led to the formation of two ionic species **B′** and **B″** (**II**, Scheme 1).

Notably, in both cases (**I**/**II**) non-classical carbenes (CAAC and Indy) were employed, which are known to be stronger σ-donors compared to classical NHCs.[9] In order to gain better insights into the factors affecting such processes, complexes of a 1,2,4-triazolin-5-ylidene, as one of the most weakly donating classical NHCs,[9b] were prepared with the objective to study, if the NHC's donating ability plays a crucial role in ligand disproportionations.

Results and discussion

Syntheses of Au(I) triazolin-5-ylidene complexes

The carbene precursor salt tazy·HCl (**1**) (Scheme 2, tazy = 4-benzyl-1-methyl-1,2,4-triazolin-5-ylidene) was readily prepared by the alkylation of 1-methyl-1,2,4-triazole, with benzyl chloride acting both as alkylating agent and solvent. The subsequent auration *via* silver carbene transfer to [AuCl(SC$_4$H$_8$)] afforded the desired Au(I) chlorido mono-carbene complex [AuCl(tazy)] (**2**) in a good yield of 78%. Initial attempts to use the same metallation route with the bromide salt tazy·HBr gave a mixture of chlorido and bromido complexes due to halido scrambling, which was corroborated by X-ray diffraction analyses (*vide infra*).

Complex **2** was isolated as white solid, which is readily soluble in common organic solvents, with exception of diethyl ether, *n*-hexane and toluene. In the ^{1}H NMR spectrum of **2** in CDCl$_3$, the benzylic protons and *N*-methyl group give singlets at 5.37 and 4.01 ppm, respectively, which show upfield shifts ($\Delta\delta$ = 0.40, 0.10 ppm) compared to those in precursor salt **1**. The formation of **2** was further corroborated by the disappearance of the resonance at 11.61 ppm attributed to the acidic proton on C5 in **1**, and the presence of a carbene signal at 174.8 ppm in the ^{13}C NMR spectrum. This carbene resonance is found to be comparable to those of previously reported Au(I) mono-(1,2,4-triazolin-5-ylidene) analogues.[10] The ESI mass spectrum of **2** displays a base peak at *m*/*z* 402 arising from $[M - Cl + CH_3OH]^+$.

The chlorido complex **2** can serve as the precursor for further ligand replacement reactions. Treating **2** with excess LiBr in acetone gave bromido complex [AuBr(tazy)] (**3**) and Finkelstein reaction with NaI led to the formation of iodido analogue [AuI(tazy)] (**4**) in good yields of 81% and 88%, respectively (Scheme 3).

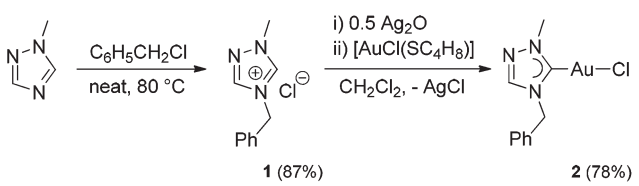

Scheme 2 Synthesis of Au(I) chlorido mono-carbene complex **2**.

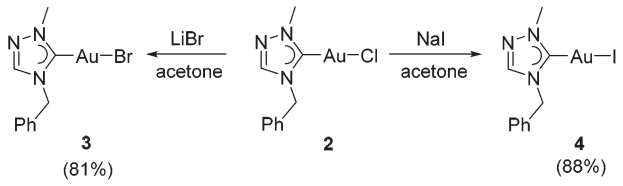

Scheme 3 Syntheses of Au(I) bromido and iodido complexes **3** and **4**.

The solubilities of complexes **3** and **4** are similar to that of precursor **2**. The ^{1}H NMR spectra of **3** and **4** in CDCl$_3$ resemble that of complex **2** and thus are non-indicative for these halido substitution reactions. However, in their ^{13}C NMR spectra, the carbene signals of **3** and **4** are found to be highly sensitive to the *trans*-standing halido ligands. Complexes **2**–**4** show a gradual downfield shift of the $^{13}C_{carbene}$ signal in the order 174.8 ppm (Cl) < 178.3 ppm (Br) < 184.8 ppm (I), which correlates to the increasing net donating ability of the *trans* halido ligands. This is in line with the earlier studies from Baker *et al.*[11] and our group,[9b,c,12] which revealed that an increased Lewis acidity of the metal center will result in an upfield $^{13}C_{carbene}$ shift. The formation of complexes **2** and **3** was also supported by their ESI-MS spectra, where dominant peaks at *m*/*z* 543 corresponding to the monocationic species $[Au(tazy)_2]^+$ were observed.

The identity of complexes **2** and **3** was confirmed by X-ray diffraction analysis on single crystals obtained by slow evaporation of their concentrated solutions in CH_2Cl_2–*n*-hexane. The molecular structures are depicted in Fig. 1. The Au–$C_{carbene}$ distance of **3** is found to be longer than that of complex **2**, which is due to the stronger *trans* influence of the bromido *versus* the chlorido ligand. As anticipated, the two benzyl substituents bend away from the coordination spheres to reduce steric repulsion. In both cases of **2** and **3**, two mono-carbene molecules were found to dimerize in an antiparallel eclipsed manner through aurophilic interactions clearly indicated by the inter-gold distances of 3.389 Å (**2**) and 3.305 Å (**3**), respect-

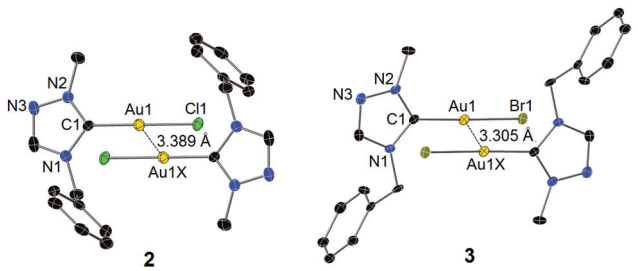

Fig. 1 Molecular structures of **2** (left) and **3** (right) showing 50% probability ellipsoids. The other crystallographically independent molecule without aurophilic interactions observed in the solid state of **3** is not shown. Hydrogen atoms and a partial bromido ligand (19%) also found in the structure of **2** have been omitted for clarity. Selected bond lengths (Å) and bond angles (°) for complex **2**: Au1–C1 1.970(3), Au1–Cl1 2.274(7), Au1–Au1X 3.389; C1–Au1–Cl1 179.9(3), N2–C1–N1 103.6(3), C1–Au1–Au1X 83.48, Cl1–Au1–Au1X 96.42. **3**: Au1–C1 1.989(4), Au1–Br1 2.4057(5), Au1–Au1X 3.305; C1–Au1–Br1 176.15(10), N2–C1–N1 103.9(3), C1–Au1–Au1X 77.61, Br1–Au1–Au1X 106.23.

ively.[13] A computational study by Pyykkö *et al*. on the dimerization of model complex [AuX(PH_3)] (X = anionic ligand) concluded that a "*softer*" anionic ligand X leads to a *stronger* aurophilic bonding.[14] In the present cases with NHCs as supporting ligands, a shorter inter-gold separation (*i.e.* stronger aurophilic interaction) was also found in complex **3**, where the bromido is "*softer*" compared to the chlorido coligand in the corresponding complex **2**. Notably, a deviation of the C1–Au1–Br1 vector from linearity was observed in the case of **3**, while the Au(I) centre of complex **2** adopts an essentially linear geometry.

Single crystals of iodido complex **4** suitable for X-ray diffraction study were obtained by slow evaporation of a concentrated solution of **4** in CH_2Cl_2. In contrast, the molecular structure was found to be the complex salt [Au(tazy)$_2$][AuI_2] (**4′**), indicating a ligand disproportionation of neutral complex **4**. The ion pair depicted in Fig. 2 contains bis(carbene) $[Au(tazy)_2]^+$ as the cationic fragment and $[AuI_2]^-$ as the counteranion. Notably, both Au(I) centers adopt a perfectly linear coordination geometry. The ions aggregate in a staggered orientation with a C1–Au1–Au2–I1 torsion angle of ~81°, leading to the formation of a polymeric array of "crossed-sticks" with an inter-gold contact of 3.316 Å.

X-ray powder diffraction was carried out to study the bulk of the crystalline material obtained from the CH_2Cl_2 solution of **4**. The experimental diffraction pattern is in very good agreement with the simulated one based on the molecular structure of **4′** (Fig. 3), confirming that **4′** indeed represents the whole solid material. Nevertheless, it should also be noted that the neutral complex **4** may only undergo ligand disproportionation yielding the ionic isomer **4′** upon crystallization. This disproportionation behavior is similar to the one that has been investigated for an indazole-derived carbene complex [AuI(Indy)].[8b]

The $C_{carbene}$ signal of the tazy ligand is a diagnostic tool to distinguish tazy-containing complexes with different coligands (*vide supra*). Thus, to identify the prevalent species present in the solution, Au(I) bis(carbene) complex [Au(tazy)$_2$]-PF_6 (**6**) was synthesized for comparison *via* a two-step protocol (Scheme 4). In the first step, the chlorido ligand of complex **2** was substituted by an acetato ligand with AgOAc. The obtained

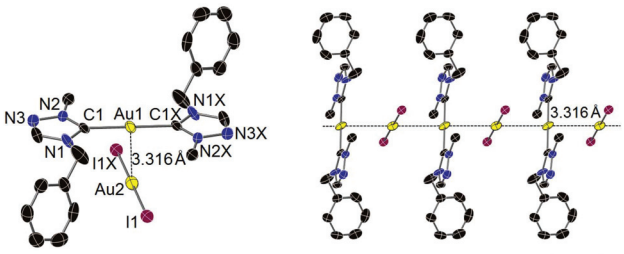

Fig. 2 Molecular structure (left) and packing pattern (right) of **4′** showing 50% probability ellipsoids. Hydrogen atoms have been omitted for clarity. Selected bond lengths (Å) and bond angles (°): Au1–C1 2.024 (5), Au2–I1 2.5586(4), Au1–Au2 3.3161(3); C1–Au1–C1X 180.0(3), I1–Au2–I1X 180.000(1), N2–C1–N1 104.3(4), C1–Au1–Au2 94.81(14), C1X–Au1–Au2 85.19(14), I1–Au2–Au1 83.545(9), I1X–Au2–Au1 96.455(9).

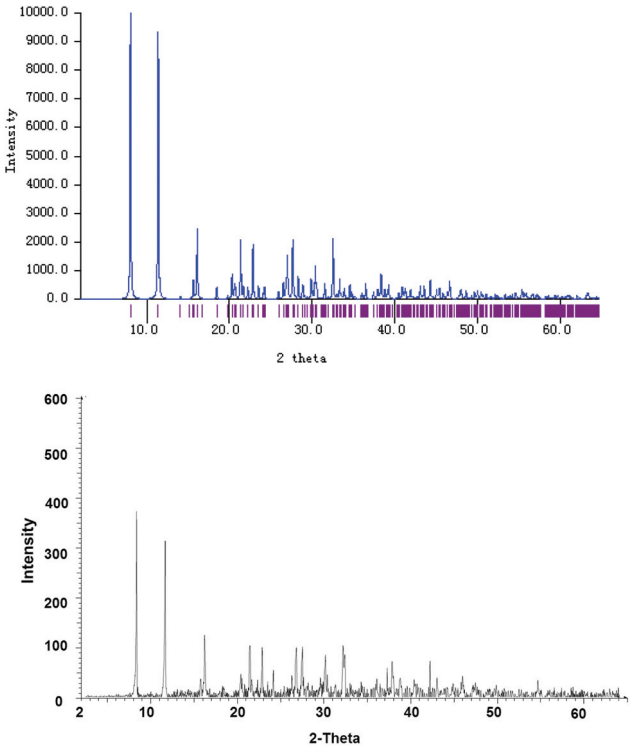

Fig. 3 Simulated (top) and experimentally determined (bottom) X-ray powder diffraction patterns of bulk crystalline solids obtained from a saturated CH_2Cl_2 solution of complex **4**.

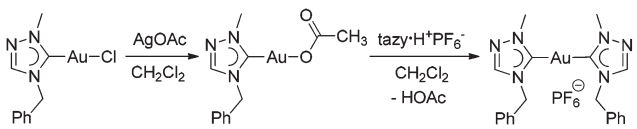

Scheme 4 Syntheses of Au(I) acetato complex **5** and bis(NHC) complex **6**.

acetato complex [Au(CH_3COO)(tazy)] (**5**) can serve as a basic precursor, which reacted with azolium salt tazy·HPF_6 and gave the desired bis(NHC) complex **6** in a good yield of 88%.

The solubilities of complexes **5** and **6** are very similar to that of the precursor **2**. Their ^{1}H NMR spectra also resemble that of **2** apart from the additional signals due to the acetato group in the case of **5**. Again, the formation of **5** and **6** was better evidenced by their ^{13}C NMR spectra, where the carbene resonances are found to shift markedly upfield ($\Delta\delta$ = 6.8 ppm, **5**) and downfield ($\Delta\delta$ = 11.4 ppm, **6**), respectively.

Single crystals of **5** and **6** for X-ray diffraction studies were obtained by slow evaporation of their concentrated CH_2Cl_2–*n*-hexane solutions. The molecular structures are shown in Fig. 4. In the structure of complex **5**, the acetato moiety is coordinated to the Au(I) center in a monodentate fashion. In contrast to the chlorido and bromido counterparts **2** and **3** (*vide supra*), a weaker aurophilic interaction with a longer inter-gold separation of 3.471 Å was observed. This is again due to the increased "*hardness*" of acetato *versus* chlorido/bromido

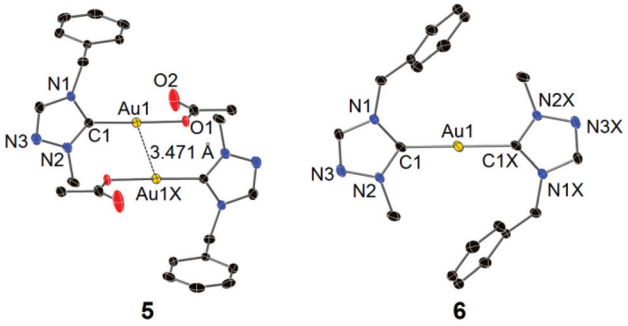

Fig. 4 Molecular structures of **5** (left) and **6** (right) showing 50% probability ellipsoids. Hydrogen atoms and solvent molecules are omitted for clarity. Selected bond length (Å) and angles (°) for complex **5**: Au1–C1 1.981(4), Au1–O1 2.039(3); C1–Au1–O1 178.12(13), N2–C1–N1 104.6(3). **6**: Au1–C1 2.017(4), C1–Au1–C1X 180.0(2), N2–C1–N1 103.2(3).

ligands (*vide supra*). In contrast to **5**, no aurophilic interaction was found in complex **6**, which likely results from the high steric demand of the two tazy ligands.

Comparison of diagnostic ^{13}C NMR spectroscopic data

The carbene resonances of complexes **2–6** are illustrated in Fig. 5. It was found that the $^{13}C_{carbene}$ signal of the fixed tazy ligand correlates well with the net donating ability of the *trans*-standing ligand. The weakest donor, the acetato ligand, leads to the most upfield shift of the tazy carbene resonance, whereas the carbene signal of bis(carbene) complex **6** bearing an additional strong carbene ligand in the *trans* position is the most downfield. This observation is in line with previous reports.[9b,c,11,12]

Notably, the $^{13}C_{carbene}$ (tazy) signal of bis(NHC) complex **6** at 186.2 ppm shows a clear downfield shift compared to resonance observed in complex **4** (184.8 ppm), which suggests that the mono-carbene complex is the prevalent species in solution. When **4′** was redissolved in $CDCl_3$ and subjected to NMR spectroscopic analysis, the same spectroscopic features were observed as for the freshly prepared complex **4**, which supports a full reversibility of the ligand disproportionation process.

UV-Vis absorption spectroscopy

To provide additional evidence that complex **4** is the prevalent species in solution instead of **4′**, UV-Vis absorption spectroscopic analyses were performed. The absorption spectra of

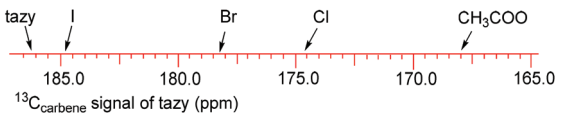

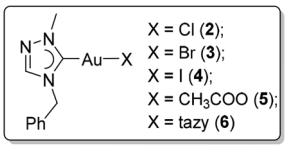

Fig. 5 ^{13}C carbene signals of tazy ligand in complexes **2–6**.

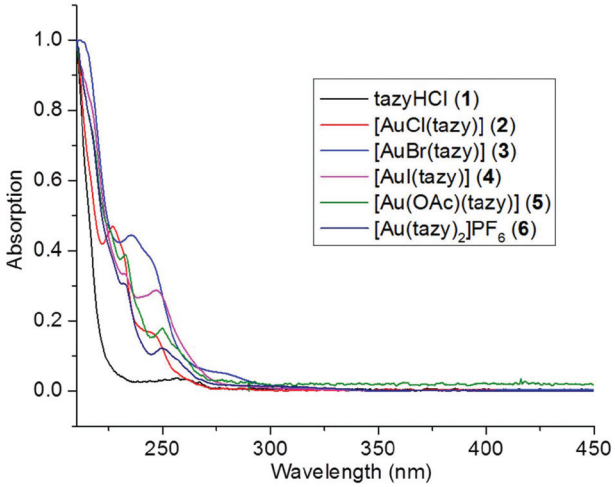

Fig. 6 Normalized absorption spectra of precursor salt **1** and complexes **2–6**.

dihalido aurate species $[AuX_2]^-$ (X = Cl, Br, I) have been thoroughly studied by Mason *et al.*[15] It has been disclosed that the $[AuI_2]^-$ anion features a characteristic LMCT band at 362 nm, which is a good indicator for the presence of $[AuI_2]^-$-containing species (such as **4′**) in solution. As shown in Fig. 6, the absorption patterns of complexes **2–6** are quite similar and all absorption bands are within the high-energy region (λ < 300 nm). Notably, in the case of iodido complex **4**, no LMCT absorption at *ca.* 362 nm characteristic for diiodidoaurate(I) is observed, which suggests the absence of the ionic species **4′** in solution.

Oxidative addition

The identity of mono-carbene species **4** in solution can be also indirectly verified by its further transformation. The oxidative addition of I_2 to complex **4** afforded the triiodido(mono-carbene) complex $[AuI_3(tazy)]$ (**7**) in a very good yield of 93% (Scheme 5).

Complex **7** was isolated as dark-red solid. The color originates most likely from the ligand-to-metal-charge-transfer (LMCT) from a iodido ligand to the d^8 Au(III) center.[12a] The formation of **7** was corroborated by its ESI mass spectrum, where a base peak at *m*/*z* 797 assignable to $[M - I + tazy]^+$ was observed. The ^{1}H NMR spectrum of **7** does not show pronounced differences despite the increased Lewis acidity of the metal center upon oxidation. Nevertheless, the $C_{carbene}$ signal is again a good indicator for the successful oxidation. This resonance has shifted significantly upfield ($\Delta\delta$ = 21.8 ppm) compared to that in Au(I) precursor **4**.

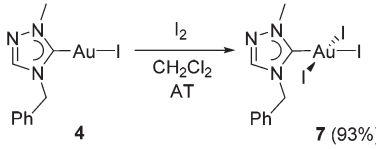

Scheme 5 Synthesis of Au(III) triiodido complex **7**.

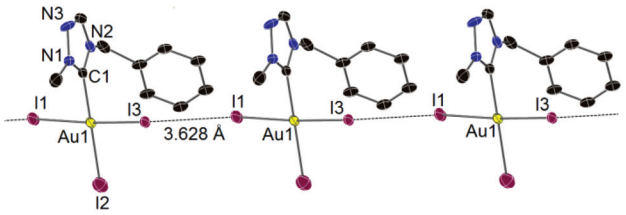

Fig. 7 Molecular structure and packing pattern of **7** showing 50% probability ellipsoids. Solvent molecules, disordered atoms are omitted for clarity. Selected bond length (Å) and angles (°): Au1–C1 2.038(11), Au1–I2 2.5888(10), Au1–I1 2.6183(8), Au1–I3 2.6259(7); C1–Au1–I2 177.1(3), I1–Au1–I3 173.26(3), C1–Au1–I1 85.8(3), C1–Au1–I3 88.9(3), I2–Au1–I1 92.27(3), I2–Au1–I3 93.11(3).

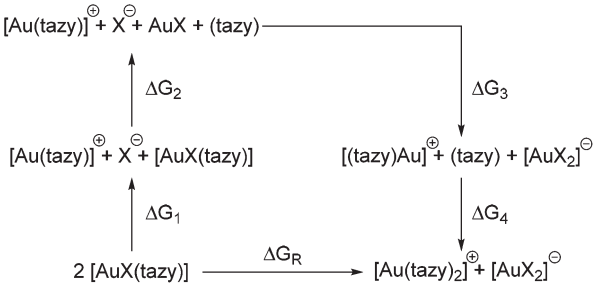

Scheme 6 Ligand redistribution process and decomposition into individual steps.

X-ray diffraction study on single crystals obtained from a concentrated CH_2Cl_2–*n*-hexane solution of **7** confirmed the essentially square planner geometry adopted by the Au(III) center (Fig. 7). No adduct of complex **7** with I_2 was found in the solid state molecular structure, which was previously observed for Au(I) phosphine analogues reported by Schmidbaur *et al.*[16] The molecules of **7** were found to aggregate through an inter-iodine contact of 3.628 Å, which is within the sum of van der Waals radii for two iodine atoms (3.80 Å).[17] The two *cis*-standing iodido ligands (I1, I3) bend to the more bulky tazy ligand with a I1–Au1–I3 bond angle of 173.26(3)°. Similar bending has been reported for a number of trihalido Au(III) carbene complexes,[8b,12] which has been attributed to the electron donation of *cis*-halido ligand to the formally vacant p_π orbital at the $C_{carbene}$ atom, and the electrostatic repulsion between the *trans*- and *cis*-halido ligands. Another interesting feature in the structure of **7** is that the Au1–I2 bond distance is shorter compared to those of Au1–I1 and Au1–I3 bonds. In earlier studies on complexes of the type $[AuX_3(NHC)]$ (X = halido ligand), the more strongly donating carbene ligand always has a greater *trans* influence and lengthens the Au–X_{trans} bond.[12a,18] In the present case, the weakening of the Au–X_{cis} bond is likely to be due to the intermolecular I–I interaction (*vide supra*).

Computational study

To gain further insight into the factors contribution or hampering ligand redistribution, the process was studied in greater detail by means of DFT calculations. The reaction between two molecules of [AuX(tazy)] can be formally decomposed into two bond-breaking and two bond-making steps, each of which contributes to the overall Gibbs free energy of the reaction (Scheme 6). While this decomposition most likely does not reflect the actual mechanism of the ligand redistribution process, it allows gauging the energetic contributions each broken and newly formed bond makes towards the overall Gibbs free energy.

The geometries of all species involved in this hypothetical reaction outlined in Scheme 6 were optimised at the B3LYP/cc-pVDZ-(PP) level of theory. Initially, no solvent model was included in the optimization, but it became quickly apparent that this leads to a vast overestimation of the charge-separation step contributing to ΔG_1. To mitigate this problem, a polarizable continuum model for dichloromethane, the solvent in which the ligand redistribution was observed, was included in the calculations.[19]

The optimized geometries are in good agreement with the molecular structures obtained by X-ray diffraction, insofar the latter are available. Bond angles and lengths are accurately reproduced, with Au–X and Au–C bonds being overestimated in the theoretical structures by less than 3%. The largest deviations were observed for species, which exhibit strong aurophilic interactions in the solid state. These are absent in the theoretical structures, explaining the slight changes in bond lengths and angles.

Regardless of the halido ligand, all reactions were found to be endothermic (Table 1). However, it should be noted that the energetic contributions from ion pairing and aurophilic interactions have not been accounted for. Aurophilic interactions can contribute up to 60 kJ mol^{-1} in additional stabilization, depending on the exact nature of the species involved,[13,20] which is sufficient for the ligand redistribution to proceed upon crystallization.[21]

The calculated energy difference between **4** and **4′** is by ~12 kJ mol^{-1} smaller for the iodido complexes when compared to the chlorido and bromido congeners, and aurophilic interactions are known to increase with softer coligands such as iodido. Hence it is very plausible that aurophilic interactions can offset the energy difference between **4** and **4′** in the solid state, while allowing the system to revert back to the mono-NHC form in solution. The larger energy difference and the weaker aurophilic interactions prevent a similar equilibrium for **2** and **3**.

When examining the individual energetic contributions in detail, it becomes apparent that cleaving the Au–X bond in **2**–**4**

Table 1 ΔG_R of the redistribution and contributions of each bond, energies in kJ mol^{-1}

	X = Cl	X = Br	X = I
ΔG_1	215.5	213.5	157.9
ΔG_2	230.0	223.0	204.3
ΔG_3	−183.7	−171.7	−112.3
ΔG_4	−205.3	−205.3	−205.3
ΔG_R	56.8	59.0	44.5

requires considerably less energy for the iodido ligand than for the lighter homologues (ΔG_1). The more polarizable iodide is a better leaving group than the harder bromide and chloride anions. However, this energetic difference is negated by a lower energy gain from aurate formation (ΔG_3) due to the stronger *trans*-influence of the iodido ligands. This stronger *trans*-influence also makes the cleavage of the Au–C bond in **2–4** less endothermic for **4** (ΔG_2), and indeed, it is energetically more favourable for the tazy ligand to bind to $[Au(tazy)]^+$ than to AuI, while this is not the case for AuCl and AuBr.

Based on these results, it appears that the combination of a stronger aurophilic interaction in the solid state of **4′** and the stronger *trans*-influence of the iodido ligand in **4** renders the ligand redistribution energetically favorable upon crystallization, while the absence of aurophilic interaction in solution explains the reversible behavior observed upon dissolving the crystalline sample. Nevertheless, it must be noted that our calculation can only address (i) electronic effects of the ligands and (ii) solvent effects as two important factors contributing to the observed ligand disproportionation upon crystallization. The crystal lattice energy as the third major contributor, on the other hand, can currently not be accounted for within the scope of this study. Hence, this study provides a deeper insight into this phenomenon, but an exact prediction of the process is expectedly not possible.

Conclusions

Four mono-NHC complexes of the type [AuX(tazy)] (X = Cl, Br, I, OAc) have been synthesized and fully characterized. Only the iodido complex underwent a reversible ligand redistribution upon crystallization. By careful analysis of crystallographic data as well as NMR and UV-Vis spectroscopic data and comparison with spectra obtained from reference compound $[Au(tazy)_2]PF_6$ (**6**), it could be firmly established that the solid phase of the iodido complex exists exclusively as the disproportionated material **4′**, while in solution the neutral form **4** is prevalent. Unlike previous reports of such redistributions, which occurred with unusually electron-rich NHC ligands, we used the weakly donating tazy ligand, thus ruling out a strong electron donor as requirement for such reactions. By contrast, a soft halido coligand with high *trans*-influence seems to be required for the reaction to proceed in this system, as evidenced by DFT calculations.

Experimental section

General considerations

Unless otherwise noted all operations were performed without taking precautions to exclude air and moisture. All solvents and chemicals were used as received without any further treatment if not noted otherwise. $[AuCl(SC_4H_8)]$ was synthesized according to the reported procedure.[22] ^1H, ^{13}C, ^{19}F and ^{31}P NMR spectra were recorded on a Bruker ACF 300 and Bruker AMX 500 spectrometer and the chemical shifts (δ) were internally referenced to the residual solvent signals relative to $[Si(CH_3)_4]$ (^1H, ^{13}C) or externally to CF_3CO_2H (^{19}F) and 85% H_3PO_4 (^{31}P). ESI mass spectra were measured using a Finnigan MAT LCQ spectrometer. Elemental analyses were carried out on a Elementar Vario Micro Cube elemental analyzer at the Department of Chemistry, National University of Singapore. UV–Vis absorption spectroscopic analyses were carried out with a Shimadzu 2550 UV-Vis spectrometer. The measurement was performed using a 0.05 mM solution in CH_3CN in a UV quartz cuvette. X-ray powder diffraction analyses were carried out with a Bruker D8 ADVANCE Powder X-ray diffractometer. 4-Benzyl-1-methyl-1,2,4-triazolium hexafluorophosphate was synthesized *via* a salt metathesis reaction of its chloride analogue and KPF_6 in H_2O.

4-Benzyl-1-methyl-1,2,4-triazolium chloride (1). 1-Methyl-1,2,4-triazole (415 mg, 5 mmol) and benzyl chloride (3 mL, 26 mmol) were mixed in a Schlenk flask. The reaction mixture was heated at 80 °C for 1 d. All the volatiles were removed *in vacuo*, and the residue was washed with diethyl ether affording the product as a hydroscopic white solid (912 mg, 4.35 mmol, 87%). ^1H NMR (500 MHz, $CDCl_3$): δ 11.61 (s, 1 H, NC^5HN), 9.28 (s, 1 H, NC^3HN), 7.60–7.58 (m, 2 H, Ar–H), 7.27–7.26 (m, 3 H, Ar–H), 5.77 (s, 2 H, NCH_2), 4.11 (s, 3 H, NCH_3). $^{13}C\{^1H\}$ NMR (125 MHz, $CDCl_3$): δ 144.7 (NC^5HN), 143.9 (NC^3HN), 133.2, 130.2, 130.0, 129.9 (Ar–C), 52.2 (NCH_2), 39.9 (NCH_3). MS (ESI): m/z 174 $[M - Cl]^+$.

4-Benzyl-1-methyl-1,2,4-triazolium bromide. This compound was synthesized in analogy to salt **1** but using benzyl bromide as the alkylating agent. The product was isolated as an off-white solid in a yield of 93%. ^1H NMR (500 MHz, $CDCl_3$): δ 11.32 (s, 1 H, NC^5HN), 9.00 (s, 1 H, NC^3HN), 7.61–7.59 (m, 2 H, Ar–H), 7.34–7.32 (m, 3 H, Ar–H), 5.79 (s, 2 H, NCH_2), 4.16 (s, 3 H, NCH_3). $^{13}C\{^1H\}$ NMR (125 MHz, $CDCl_3$): δ 144.3 (NC^5HN), 143.7 (NC^3HN), 132.8, 130.4, 130.2, 130.0 (Ar–C), 52.5 (NCH_2), 40.2 (NCH_3). MS (ESI): m/z 174 $[M - Br]^+$.

Chlorido(4-benzyl-1-methyl-1,2,4-triazolin-5-ylidene)gold(I) (2). Triazolium salt **1** (210 mg, 1 mmol) and Ag_2O (128 mg, 0.55 mmol) were mixed in a 50 mL round bottom flask. CH_2Cl_2 (10 mL) was then added, and the reaction mixture was stirred in dark at ambient temperature for 3 h. The resulting suspension was then directly transferred into the solution of $[AuCl(SC_4H_9)]$ (320 mg, 1 mmol) in CH_2Cl_2 (10 mL). The reaction mixture was then stirred overnight. All insoluble material was filtered off through Celite, and the filtrate was dried *in vacuo* affording the product as a white solid (316 mg, 0.78 mmol, 78%). ^1H NMR (500 MHz, $CDCl_3$): δ 7.97 (s, 1 H, NCHN), 7.39–7.34 (m, 5H, Ar–H), 5.37 (s, 2 H, NCH_2), 4.01 (s, 3 H, NCH_3). $^{13}C\{^1H\}$ NMR (125 MHz, $CDCl_3$): 174.8 (s, NCN), 142.5, 134.1, 130.1, 130.0, 129.0 (Ar–C), 53.4 (NCH_2), 40.9 (s, NCH_3). Anal. Calcd for $C_{10}H_{11}AuClN_3$: C, 29.61; H, 2.73; N, 10.36%. Found: C, 29.84; H, 2.69; N, 10.24%. MS (ESI): m/z 402 $[M - Cl + CH_3OH]^+$.

Bromido(4-benzyl-1-methyl-1,2,4-triazolin-5-ylidene)gold(I) (3). Complex **2** (203 mg, 0.5 mmol) and LiBr (434 mg, 5 mmol) were mixed in a 50 mL round bottom flask. Acetone

(15 mL) was added, and the reaction mixture was stirred at ambient temperature for 1 d. All the volatiles were removed *in vacuo* and CH_2Cl_2 (15 mL) was added to the residue. The resulting suspension was filtered through Celite, and the filtrate was dried *in vacuo*. Column chromatography (SiO_2) afforded the product as off-white powder (182 mg, 0.41 mmol, 81%). ^{1}H NMR (500 MHz, $CDCl_3$): δ 7.93 (s, 1 H, NCHN), 7.41–7.35 (m, 5 H, Ar–H), 5.39 (s, 2 H, NCH_2), 4.04 (s, 3 H, NCH_3). $^{13}C\{^1H\}$ NMR (125 MHz, $CDCl_3$): δ 178.3 (NCN), 142.3, 134.0, 130.2, 130.1, 129.1 (Ar–C), 53.4 (NCH_2), 40.9 (NCH_3). Anal. Calcd for $C_{10}H_{11}AuBrN_3{\cdot}0.5CH_2Cl_2$: C, 25.60; H, 2.46; N, 8.53%. Found: C, 25.64; H, 2.09; N, 8.79%. MS (ESI): *m*/*z* 543 $[M - Br + tazy]^+$.

Iodido(4-benzyl-1-methyl-1,2,4-triazolin-5-ylidene)gold(I) (4). Complex **2** (203 mg, 0.5 mmol) and NaI (375 mg, 2.5 mmol) were mixed in a 50 mL round bottom flask. Acetone (15 mL) was added, and the reaction mixture was stirred at ambient temperature for 1 d. All the volatiles were removed *in vacuo* and CH_2Cl_2 (15 mL) was added to the residue. The resulting suspension was filtered through Celite, and the filtrate was dried *in vacuo* affording the product as an off-white solid (218 mg, 0.44 mmol, 88%). ^{1}H NMR (300 MHz, $CDCl_3$): δ 7.91 (s, 1 H, NCHN), 7.42–7.35 (m, 5 H, Ar–H), 5.40 (s, 2 H, NCH_2), 4.05 (s, 3 H, NCH_3). $^{13}C\{^1H\}$ NMR (75 MHz, $CDCl_3$): 184.8 (NCN), 142.2, 134.1, 130.14, 130.06, 129.1 (Ar–C), 53.3 (NCH_2), 40.8 (NCH_3). Anal. Calcd for $C_{10}H_{11}AuIN_3$: C, 24.16; H, 2.23; N, 8.45%. Found: C, 24.28; H, 2.25; N, 8.40%. MS (ESI): *m*/*z* 543 $[M - I + tazy]^+$.

Acetato(4-benzyl-1-methyl-1,2,4-triazolin-5-ylidene)gold(I) (5). Complex **2** (203 mg, 0.5 mmol) and AgO_2CCH_3 (92 mg, 0.55 mmol) were mixed in a 50 mL round bottom flask. CH_2Cl_2 (10 mL) was then added, and the reaction mixture was stirred in dark at ambient temperature for 1 h. The resulting suspension was filtered through Celite, and the filtrate was dried *in vacuo* affording the product as a white solid (152 mg, 0.35 mmol, 71%). ^{1}H NMR (300 MHz, $CDCl_3$): δ 8.03 (s, 1 H, NCHN), 7.35–7.32 (m, 5 H, Ar–H), 5.34 (s, 2 H, NCH_2), 3.96 (s, 3 H, NCH_3), 2.00 (s, 3 H, CH_3COO). $^{13}C\{^1H\}$ NMR (75 MHz, $CDCl_3$): δ 177.9 (CH_3COO), 168.0 (NCN), 142.6, 134.2, 130.0, 129.8, 129.1 (Ar–C), 53.3 (NCH_2), 40.8 (NCH_3), 24.3 (CH_3COO). Anal. Calcd for $C_{12}H_{14}AuN_3O_2$: C, 33.58; H, 3.29; N, 9.79. Found: C, 33.25; H, 3.18; N, 9.77. MS (ESI): *m*/*z* 543 $[M - CH_3COO + tazy]^+$.

Bis(4-benzyl-1-methyl-1,2,4-triazolin-5-ylidene)gold(I) hexafluoro-phosphate (6). Complex **5** (86 mg, 0.2 mmol) and 4-benzyl-1-methyl-1,2,4-triazolium hexafluorophosphate (64 mg, 0.2 mmol) were mixed in a 50 mL round bottom flask. CH_2Cl_2 (10 mL) was then added, and the reaction mixture was stirred at ambient temperature overnight. The resulting solution was concentrated and *n*-hexane was added. The precipitates were collected and dried *in vacuo* affording the product as a white solid (121 mg, 0.176 mmol, 88%). ^{1}H NMR (500 MHz, $CDCl_3$): δ 8.13 (s, 2 H, NCHN), 7.35–7.33, 7.25–7.23 (m, 10 H, Ar–H), 5.34 (s, 4 H, NCH_2), 3.99 (s, 3 H, NCH_3). $^{13}C\{^1H\}$ NMR (125 MHz, $CDCl_3$): δ 186.2 (NCN), 143.7, 135.1, 130.0, 129.7, 128.7 (Ar–C), 54.1 (NCH_2), 41.2 (NCH_3). $^{19}F\{^1H\}$ NMR (282 MHz, $CDCl_3$): δ 3.30 (d, PF_6). $^{31}P\{^1H\}$ NMR (121 MHz, $CDCl_3$): δ −143.7 (m, PF_6). Anal. Calcd for $C_{20}H_{22}AuF_6N_6P$: C, 34.90; H, 3.22; N, 12.21. Found: C, 34.66; H, 3.09; N, 12.16%. MS (ESI): *m*/*z* 543 $[M - PF_6]^+$.

Triiodido(4-benzyl-1-methyl-1,2,4-triazolin-5-ylidene) gold(III) (7). Complex **4** (99 mg, 0.2 mmol) was dissolved in CH_2Cl_2 (10 mL) and elemental iodine (64 mg, 0.25 mmol) dissolved in CH_2Cl_2 (10 mL) was added dropwise at −30 °C. The reaction mixture was stirred at −30 °C for 30 min and at ambient temperature for another 2 h. All the volatiles were removed. The residue was washed with *n*-hexane (5 mL × 3) and dried *in vacuo* affording the product as a dark-red solid (139 mg, 0.186 mmol, 93%). ^{1}H NMR (500 MHz, $CDCl_3$): δ 7.93 (s, 1 H, NCHN), 7.47–7.45 (m, 5 H, Ar–H), 5.34 (s, 2 H, NCH_2), 4.02 (s, 3H, NCH_3). $^{13}C\{^1H\}$ NMR (75 MHz, $CDCl_3$): δ 163.0 (NCN), 143.7, 130.8, 130.5, 130.2 (Ar–C), 53.8 (NCH_2), 41.1 (NCH_3). Anal. Calcd for $C_{10}H_{11}AuI_3N_3$: C, 16.00; H, 1.48; N, 5.60. Found: C, 16.45; H, 1.47; N, 5.62%. MS (ESI): *m*/*z* 543 $[M - 3I + tazy]^+$, 797 $[M - I + tazy]^+$.

X-ray diffraction studies

X-ray data for **2**, **3**, **4**, **5**·H_2O, **6** and **7** were collected with a Bruker AXS SMART APEX diffractometer, using Mo-K_α radiation at 100(2)K with the SMART suite of Programs.[23] Data were processed and corrected for Lorentz and polarisation effects with SAINT,[24] and for absorption effect with SADABS.[25] Structural solution and refinement were carried out with the SHELXTL suite of programs.[26] The structure was solved by direct methods to locate the heavy atoms, followed by difference maps for the light, non-hydrogen atoms. All non-hydrogen atoms were generally given anisotropic displacement parameters in the final model. All H-atoms were put at calculated positions.

Computational methods

All calculations were carried out using hybrid density functional theory (DFT) employing the B3LYP functional[27] and the Gaussian 09 software,[28] using the IEFPCM approach to account for solvatation in dichloromethane.[19] The nature of all stationary points was confirmed by frequency analysis, and all geometries were found to represent minima on the potential energy surface. For the optimisation of complex geometries and the calculation of their Gibbs free energies, gold and iodine were described with a cc-pVDZ-PP basis set in combination with the corresponding electronic core potential (ECP),[29] while the lighter elements were treated with the cc-pVDZ basis set.[30] The basis sets were all obtained from the EMSL Basis Set Library.[31]

Acknowledgements

We thank the National University of Singapore and the Singapore Ministry of Education for financial support (WBS

R-143-000-483-112). Technical assistance from staff at the CMMAC of our department is appreciated. In particular, we thank Ms Geok Kheng Tan, Ms Hong Yimian and Prof. Lip Lin Koh for determining the X-ray molecular structures.

Notes and references

1 For a review on coinage metal–NHCs, see: J. C. Y. Lin, R. T. W. Huang, C. S. Lee, A. Bhattacharyya, W. S. Hwang and I. J. B. Lin, *Chem. Rev.*, 2009, **109**, 3561.
2 For catalytic applications, see: (*a*) N. Marion and S. P. Nolan, *Chem. Soc. Rev.*, 2008, **37**, 1776; (*b*) J. D. Egbert, C. S. J. Cazin and S. P. Nolan, *Catal. Sci. Technol.*, 2013, **3**, 912; (*c*) S. Díez-González, N. Marion and S. P. Nolan, *Chem. Rev.*, 2009, **109**, 3612; (*d*) A. S. K. Hashmi, *Chem. Rev.*, 2007, **107**, 3180.
3 For luminescence applications, see: (*a*) L. Mercs and M. Albrecht, *Chem. Soc. Rev.*, 2010, **39**, 1903; (*b*) C. Bronner and O. S. Wenger, *Dalton Trans.*, 2011, **40**, 12409.
4 For biological applications, see: (*a*) W. Liu and R. Gust, *Chem. Soc. Rev.*, 2013, **42**, 755; (*b*) L. Oehninger, R. Rubbiani and I. Ott, *Dalton Trans.*, 2013, **42**, 3269; (*c*) A. Gautier and F. Cisnetti, *Metallomics*, 2012, **4**, 23; (*d*) C. G. Hartinger, N. Metzler-Nolte and P. J. Dyson, *Organometallics*, 2012, **31**, 5677.
5 For reviews on Ag–NHCs, see: (*a*) J. C. Garrison and W. J. Youngs, *Chem. Rev.*, 2005, **105**, 3978; (*b*) I. J. B. Lin and C. S. Vasam, *Coord. Chem. Rev.*, 2007, **251**, 642.
6 For selected examples, see: (*a*) H. M. J. Wang and I. J. B. Lin, *Organometallics*, 1998, **17**, 972; (*b*) O. Guerret, S. Solé, H. Gornitzka, M. Teichert, G. Trinquier and G. Bertrand, *J. Am. Chem. Soc.*, 1997, **119**, 6668.
7 C. Boehme and G. Frenking, *Organometallics*, 1998, **17**, 5801.
8 (*a*) G. D. Frey, R. D. Dewhurst, S. Kousar, B. Donnadieu and G. Bertrand, *J. Organomet. Chem.*, 2008, **693**, 1674; (*b*) H. Sivaram, R. Jothibasu and H. V. Huynh, *Organometallics*, 2012, **31**, 1195.
9 (*a*) V. Lavallo, Y. Canac, C. Präsang, B. Donnadieu and G. Bertrand, *Angew. Chem., Int. Ed.*, 2005, **44**, 5705; (*b*) H. V. Huynh, Y. Han, R. Jothibasu and J. A. Yang, *Organometallics*, 2009, **28**, 5395; (*c*) S. Guo, H. Sivaram, D. Yuan and H. V. Huynh, *Organometallics*, 2013, **32**, 3685.
10 H. M. J. Wang, C. S. Vasam, T. Y. R. Tsai, S.-H. Chen, A. H. H. Chang and I. J. B. Lin, *Organometallics*, 2005, **24**, 486.
11 M. V. Baker, P. J. Barnard, S. K. Brayshaw, J. L. Hickey, B. W. Skelton and A. H. White, *J. Chem. Soc., Dalton Trans.*, 2005, 37.
12 (*a*) H. V. Huynh, S. Guo and W. Wu, *Organometallics*, 2013, **32**, 4591; (*b*) J. C. Bernhammer and H. V. Huynh, *Dalton Trans.*, 2012, **41**, 8600.
13 For reviews on aurophilic interactions, see: (*a*) H. Schmidbaur, *Chem. Soc. Rev.*, 1995, **24**, 391; (*b*) H. Schmidbaur, *Gold Bulletin*, 2000, **33**, 1; (*c*) H. Schmidbaur and A. Schier, *Chem. Soc. Rev.*, 2012, **41**, 370.
14 P. Pyykkö, N. Runeberg and F. Mendizabal, *Chem. – Eur. J.*, 1997, **3**, 1451.
15 (*a*) M. M. Savas and W. R. Mason, *Inorg. Chem.*, 1987, **26**, 301; (*b*) M. E. Koutek and W. R. Mason, *Inorg. Chem.*, 1980, **19**, 648.
16 D. Schneider, O. Schuster and H. Schmidbaur, *Dalton Trans.*, 2005, 1940.
17 P. H. Svensson and L. Kloo, *Chem. Rev.*, 2003, **103**, 1649.
18 (*a*) P. de Frémont, R. Singh, E. D. Stevens, J. L. Petersen and S. P. Nolan, *Organometallics*, 2007, **26**, 1376; (*b*) S. Gaillard, A. M. Z. Slawin, A. T. Bonura, E. D. Stevens and S. P. Nolan, *Organometallics*, 2010, **29**, 394.
19 J. Tomasi, B. Mennucci and R. Cammi, *Chem. Rev.*, 2005, **105**, 2999.
20 (*a*) P. Pyykkö, *Chem. Rev.*, 1997, **97**, 597; (*b*) H. Schmidbaur, S. Cronje, B. Djordjevic and O. Schuster, *Chem. Phys.*, 2005, **311**, 151; (*c*) H. Schmidbaur and A. Schier, *Chem. Soc. Rev.*, 2008, **37**, 1931; (*d*) A. Otero-de-la-Roza, J. D. Mallory and E. R. Johnson, *J. Chem. Phys.*, 2014, **140**, 18A504.
21 P. Pyykkö, W. Schneider, A. Bauer, A. Bayler and H. Schmidbaur, *Chem. Commun.*, 1997, 1111.
22 (*a*) R. Usón, A. Laguna and M. Laguna, *Inorg. Synth.*, 1989, **26**, 85; (*b*) M.-C. Brandys, M. C. Jennings and R. J. Puddephatt, *J. Chem. Soc., Dalton Trans.*, 2000, 4601.
23 *SMART version 5.628*, Bruker AXS Inc., Madison, WI, 2001.
24 *SAINT+ version 6.22a*, Bruker AXS Inc., Madison, WI, 2001.
25 G. W. Sheldrick, *SADABS version 2.10*, University of Göttingen, 2001.
26 *SHELXTL version 6.14*, Bruker AXS Inc., Madison, WI, 2000.
27 (*a*) A. D. Becke, *J. Chem. Phys.*, 1993, **98**, 5648; (*b*) A. D. Becke, *Phys. Rev. A*, 1988, **38**, 3098; (*c*) C. Lee, W. Yang and R. G. Parr, *Phys. Rev. B: Condens. Matter*, 1988, **37**, 785.
28 M. J. Frisch, G. W. Trucks, H. B. Schlegel, G. E. Scuseria, M. A. Robb, J. R. Cheeseman, G. Scalmani, V. Barone, B. Mennucci, G. A. Petersson, H. Nakatsuji, M. Caricato, X. Li, H. P. Hratchian, A. F. Izmaylov, J. Bloino, G. Zheng, J. L. Sonnenberg, M. Hada, M. Ehara, K. Toyota, R. Fukuda, J. Hasegawa, M. Ishida, T. Nakajima, Y. Honda, O. Kitao, H. Nakai, T. Vreven, J. A. Montgomery Jr., J. E. Peralta, F. Ogliaro, M. Bearpark, J. J. Heyd, E. Brothers, K. N. Kudin, V. N. Staroverov, T. Keith, R. Kobayashi, J. Normand, K. Raghavachari, A. Rendell, J. C. Burant, S. S. Iyengar, J. Tomasi, M. Cossi, N. Rega, J. M. Millam, M. Klene, J. E. Knox, J. B. Cross, V. Bakken, C. Adamo, J. Jaramillo, R. Gomperts, R. E. Stratmann, O. Yazyev, A. J. Austin, R. Cammi, C. Pomelli, J. W. Ochterski, R. L. Martin, K. Morokuma, V. G. Zakrzewski, G. A. Voth, P. Salvador, J. J. Dannenberg, S. Dapprich, A. D. Daniels, O. Farkas, J. B. Foresman, J. V. Ortiz, J. Cioslowski and D. J. Fox, *Gaussian 09, Revision B.01*, Gaussian, Inc., Wallingford CT, 2010.

29 (*a*) K. A. Peterson, D. Figgen, E. Goll, H. Stoll and M. Dolg, *J. Chem. Phys.*, 2003, **119**, 11113; (*b*) K. A. Peterson, *J. Chem. Phys.*, 2003, **119**, 11099; (*c*) D. Figgen, G. Rauhut, M. Dolg and H. Stoll, *Chem. Phys.*, 2005, **311**, 227; (*d*) K. A. Peterson and C. Puzzarini, *Theor. Chem. Acc.*, 2005, **114**, 283; (*e*) K. A. Peterson, B. C. Shepler, D. Figgen and H. Stoll, *J. Phys. Chem. A*, 2006, **110**, 13877.

30 (*a*) T. H. Dunning Jr., *J. Chem. Phys.*, 1989, **90**, 1007; (*b*) D. E. Woon and T. H. Dunning Jr., *J. Chem. Phys.*, 1993, **98**, 1358.

31 (*a*) D. Feller, *J. Comput. Chem.*, 1996, **17**, 1571; (*b*) K. L. Schuchardt, B. T. Didier, T. Elsethagen, L. Sun, V. Gurumoorthi, J. Chase, J. Li and T. L. Windus, *J. Chem. Inf. Model.*, 2007, **47**, 1045.